RESEARCH COMMUNICATION

Inhibitor of differentiation 4 drives brain tumor-initiating cell genesis through cyclin E and notch signaling

Hye-Min Jeon,[1] Xun Jin,[1] Joong-Seob Lee,[1] Se-Yeong Oh,[1] Young-Woo Sohn,[1] Hyo-Jung Park,[1] Kyeung Min Joo,[2] Woong-Yang Park,[3] Do-Hyun Nam,[2] Ronald A. DePinho,[4] Lynda Chin,[4] and Hyunggee Kim[1,5]

[1]School of Life Sciences and Biotechnology, Korea University, Seoul 136-713, Republic of Korea; [2]Department of Neurosurgery, Sungkyunkwan University School of Medicine, Seoul 135-710, Republic of Korea; [3]Department of Biochemistry and Molecular Biology, Seoul National University School of Medicine, Seoul 110-799, Republic of Korea; [4]Department of Medical Oncology and Center for Applied Cancer Science, Belfer Institute for Innovative Cancer Science, Dana-Farber Cancer Institute, Harvard Medical School, Boston, Massachusetts 02115, USA

Cellular origins and genetic factors governing the genesis and maintenance of glioblastomas (GBM) are not well understood. Here, we report a pathogenetic role of the developmental regulator Id4 (inhibitor of differentiation 4) in GBM. In primary murine Ink4a/Arf$^{-/-}$ astrocytes, and human glioma cells, we provide evidence that enforced Id4 can drive malignant transformation by stimulating increased cyclin E to produce a hyperproliferative profile and by increased Jagged1 expression with Notch1 activation to drive astrocytes into a neural stem-like cell state. Thus, Id4 plays an integral role in the transformation of astrocytes via its combined actions on two-key cell cycle and differentiation regulatory molecules.

Supplemental material is available at http://www.genesdev.org.

Received March 3, 2008; revised version accepted June 16, 2008.

The self-renewal, differentiative, and proliferative states of tissue stem and progenitor cells are maintained by a variety of well-defined cell fate determinant factors (Keller 2005). Disregulation of such key developmental regulators and acquisition and maintenance of an immature differentiation phenotype are common themes across a broad spectrum of cancer types, including primary brain cancers (Garraway and Sellers 2006). Indeed, a growing body of evidence supports the view that developmental regulators play direct roles in driving aspiring cancer cells toward a malignant phenotype, one that is endowed with stem-like cell properties including robust renewal potential (Beachy et al. 2004). This cellular phenotype, embodied in the cancer stem cell paradigm (Pardal et al. 2003), has been well documented in the highly malignant brain cancer, primary glioblastoma multiforme (GBM) (Galli et al. 2004; Singh et al. 2004). The cellular origins and specific genetic elements involved in the genesis and maintenance of these so-called brain cancer stem cells (BCSCs) remain areas of intensive investigation.

[*Keywords*: Id4; Ink4a/Arf$^{-/-}$ astrocyte; notch signaling; cyclin E; neural stem-like cells; glioblastoma]
[5]Corresponding author.
E-MAIL hg-kim@korea.ac.kr; FAX 82-2-953-0737.
Article is online at http://www.genesdev.org/cgi/doi/10.1101/gad.1668708.

Results and Discussion

Id4 is overexpressed human GBM, and can drive transformation of murine Ink4a/Arf$^{-/-}$ astrocytes

Given the biological significance of stem cell fate determinants in the regulation of normal self-renewal and differentiation, we hypothesized that the genetic or epigenetic alterations in classical cell fate determinants might cooperate with prototypical oncogenes and tumor suppressor genes to both effect malignant transformation and endow stem cell-like renewal activity in these tumors (Leung et al. 2004; Ligon et al. 2007). We were particularly focused on the expression and functional activity of inhibitor of differentiation 4 (Id4) in GBM given its prominent role in governing neural stem cell (NSC) fate decisions (Yun et al. 2004).

Id4 mRNA levels were found to be increased in nine of 15 GBM samples as compared with human normal brain tissue (Supplemental Fig. S1A) and abundant Id4 mRNA and protein levels were detected in five of seven human glioma cell lines (A172, LN229, LN18, U87MG, and T98G) and an immortalized human NSC line (HB1.F3) (Cho et al. 2002), but not in the normal human astrocytes (NHA) (Supplemental Fig. S1B). Tumor microarray analysis showed 38 of 68 newly diagnosed human GBM (WHO Grade IV) specimens with robust Id4 expression with heterogenous staining patterns within the same tumor sample (Supplemental Fig. S1C). This heterogeneity and importance of Id family members in endothelial cell biology (Lyden et al. 1999) prompted coimmunofluorescence studies to evaluate expression of Id4 and the endothelial cell marker, CD31. The majority of Id4$^+$ cells were CD31$^-$ and, notably, these Id4$^+$ cells were found to reside near the vasculature—a location postulated as the preferred residence of BCSCs (Calabrese et al. 2007). In contrast, only a few Id4$^+$ cells were CD31$^+$, and most of these positive cells were associated with macrovessels in the human GBM specimens (Supplemental Fig. S2).

These expression findings raised the possibility that Id4 overexpression might be relevant to the genesis and maintenance of a large fraction of GBM cases, prompting us to determine whether enforced Id4 expression could drive malignant transformation of primary murine astrocytes derived from Ink4a/Arf$^{-/-}$, p53$^{-/-}$, or wild-type mice. Ectopic Id4 expression in Ink4a/Arf$^{-/-}$, but not wild-type or p53$^{-/-}$, astrocytes significantly accelerated cell proliferation in cell culture (Supplemental Fig. S1D; data not shown) and enabled tumor formation in vivo (n = 6 mice) (Supplemental Fig. S1E). Thus, Id4 can function as a potent oncogene in astrocytes deficient for the signature GBM tumor suppressor, Ink4a/Arf.

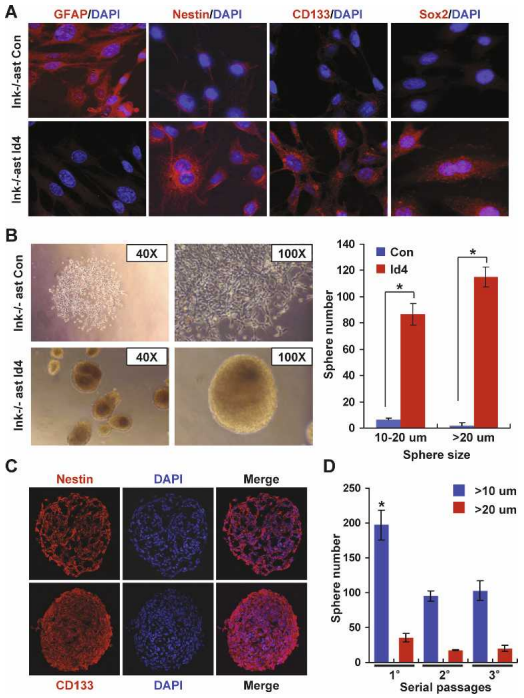

Figure 1. Conversion of Ink4a/Arf$^{-/-}$ astrocytes to neural stem-like cells by Id4. (*A*) Up-regulation of neural stem cell markers in the Id4-transduced Ink4a/Arf$^{-/-}$ astrocytes. Immunofluorescence images (400×) of GFAP (astrocyte marker), Nestin, Cd133, and Sox2 (neural stem and progenitor cell markers) in the vector-transduced Ink4a/Arf$^{-/-}$ astrocytes and Id4-transduced Ink4a/Arf$^{-/-}$ astrocytes grown in DMEM + 10% FBS culture conditions. (*B*) Neurosphere formation of Id4-transduced Ink4a/Arf$^{-/-}$ astrocytes grown in neural stem cell culture conditions (DMEM/F12 + EGF [20 ng/mL] + bFGF [20 ng/mL]). (*Left* panel) Representative photos showing vector-transduced Ink4a/Arf$^{-/-}$ astrocytes and Id4-transduced Ink4a/Arf$^{-/-}$ astrocytes grown in the neural stem cell culture for 7 d. (*Right* panel) Number of neurospheres (10–20 µm and >20 µm) of vector-transduced Ink4a/Arf$^{-/-}$ astrocytes and Id4-transduced Ink4a/Arf$^{-/-}$ astrocytes (4000 cells per 24-well plate or one cell per square millimeter) grown in neural stem cell culture for 10 d. (*) $P < 0.01$. (*C*) Representative immunofluorescence images (100×) showing Nestin and Cd133 in the cryomicrodissected neurospheres (10 µm) derived from Id4-transduced Ink4a/Arf$^{-/-}$ astrocytes. (*D*) Neurosphere formation during three serial passages of Id4-transduced Ink4a/Arf$^{-/-}$ astrocytes (4000 cells per 24-well plate) grown in neural stem cell culture for 10 d. (*) $P < 0.01$.

Id4 drives conversion of Ink4a/Arf$^{-/-}$ astrocytes into neural stem-like cells

Embryonic expression patterns of Id4 differ significantly from the other three Id family members (Id1, Id2, and Id3) in that Id4 expression is primarily restricted to the developing central nervous system (Jen et al. 1996). Disruption of the Id4 gene in mice results in neural tube proliferation defects, premature neuroblast differentiation, and overall reduction in brain size with drastic disruption in brain architecture (Bedford et al. 2005; Yun et al. 2004). Accordingly, we observed that Id4 mRNA levels are high in the developing cerebral cortex, remaining relatively constant from embryonic day 13.5 (E13.5) to E19.5, and then declining markedly in postnatal life (Supplemental Fig. S3A). This Id4 expression profile is consistent with its role as a critical regulator of NSC/progenitor cell biology and cerebral cortex development.

The defining properties of BCSCs include cancer-initiating ability upon implantation, extensive self-renewal potential, sequential neurosphere formation capacity, impaired multilineage differentiation potential, and capacity to generate nontumorigenic progeny (Vescovi et al. 2006). To assess the potential of Id4 to commandeer the mature differentiation state of astrocytes, we audited astrocyte (GFAP and S100β) and NSC (Nestin, Cd133, and Sox2) markers following transduction of Ink4a/Arf$^{-/-}$ astrocytes with vectors encoding Id4-EGFP or EGFP only (designated hereafter as Id4-transduced or vector-transduced cells). As shown in Figure 1A and Supplemental Figure S3, B and C, the expression levels of GFAP and S100β declined markedly, while all NSC markers increased dramatically in Id4-transduced Ink4a/Arf$^{-/-}$astrocytes relative to vector-transduced control cells. Furthermore, upon placement of low numbers of Id4- or vertor-transduced Ink4a/Arf$^{-/-}$ astrocytes (one cell per square millimeter at the 24-well culture plates) into NSC culture media, the former showed increased capacity to produce neurosphere-like aggregates (Fig. 1B). Specifically, 43 neurospheres were generated in 38 of 96 single-cell-seeded wells in the Id4-transduced Ink4a/Arf$^{-/-}$ astrocytes compared with seven neurospheres in 96 single-cell-seeded wells for the control cells (data not shown). Id4-transduced neurospheres possessed Nestin^{+} and Cd133^{+} cells (Fig. 1C) and exhibited self-renewal activity as single dissociated cells, i.e., these cells could be serially passaged under the NSC culture conditions (Fig. 1D). Thus, Id4 appears capable of driving Ink4a/Arf$^{-/-}$ astrocytes toward a dedifferentiated phenotype with characteristic NSC/progenitor markers and renewal activity.

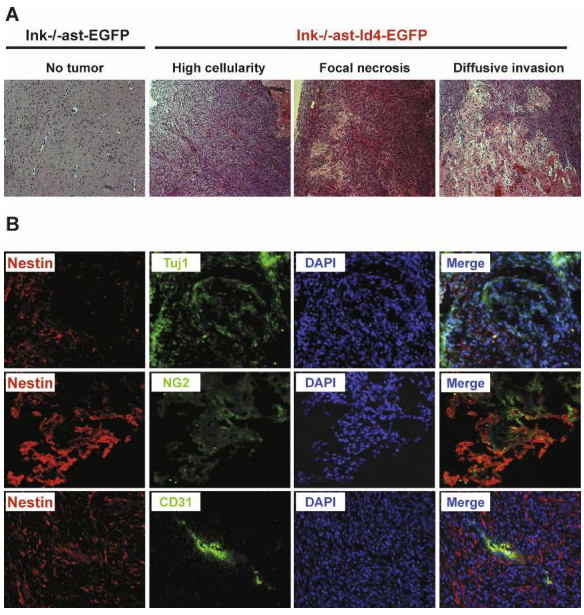

Figure 2. Gliomagenesis and in vivo differentiation of in the Id4 overexpressing Ink4a/Arf$^{-/-}$ astrocytes after intracerebral implantation. (*A*) No tumors (40× magnification from Supplemental Fig. S4A, *left* photo) observed in a nude mouse injected with Ink4a/Arf$^{-/-}$ astrocytes-Con-EGFP. Ink4a/Arf$^{-/-}$ astrocytes-Id4-EGFP-derived gliomas (40× magnification from Supplemental Fig. S4A, right photo) showing a high cellularity, focal necrosis, and diffusive invasion. (*B*) Immunofluorescence images (100×) showing Nestin^{+} cells (red) or Tuj1^{+} neuronal cells (green) or merge; Nestin^{+} cells (red) or NG2^{+} oligodendrocyte cells (green) or merge; Nestin^{+} cells (red) or CD31^{+} endothelial cells (green) or merge in brain tissues derived from orthotopically injected Ink4a/Arf$^{-/-}$ astrocytes-Id4-EGFP (brain tumor sections). Nuclei were stained with DAPI (blue).

Tumor-initiating frequency and histological characteristics of gliomas derived from Id4-transduced Ink4a/Arf$^{-/-}$ astrocytes

Next, we assessed the tumorigenic potential of limiting cell numbers following intracerebral injection and subsequent detailed clinical and histological assessment of injected brains. While no brain tumors formed with injection of 50,000 vector-transduced Ink4a/Arf$^{-/-}$ astrocytes, the same number of Id4-transduced Ink4a/Arf$^{-/-}$ astrocytes formed high-grade gliomas within 3–4 wk (n = 5 mice) (Supplemental Fig. S4A). Furthermore, three of three mice injected of 1000 Id4-transduced Ink4a/Arf$^{-/-}$ astrocytes developed tumors within 5–6 wk (data not shown), consistent with robust "tumor-initiating" potential as defined previously (Singh et al. 2004). Upon histological examination, the tumors derived from Id4-transduced Ink4a/Arf$^{-/-}$ cells possessed hallmark features of GBM including high cellularity, focal necrosis, and diffuse invasion (Fig. 2A). Thus, Id4 cooperates with Ink4a/Arf deficiency to enable primary astrocytes to attain a classical GBM phenotype.

Given the role of Id4 in neuronal differentiation, we assessed the differentiation profiles of cells or derivative tumors from orthotopically injected Id4- and vector-transduced Ink4a/Arf$^{-/-}$ astrocytes which also express EGFP. The Id4-transduced Ink4a/Arf$^{-/-}$ astrocyte-derived tumors showed many EGFP$^+$ cells which stained positive for Nestin (NSC/progenitor), Tuj1 (neuronal), or NG2 (oligodendrocyte) markers and negative for the CD31 (endothelial cell) marker (Fig. 2B for tumors derived from injection of Id4-transduced Ink4a/Arf$^{-/-}$ astrocytes; Supplemental Figs. S4B for EGFP, S5A for brain injected with vector-transduced Ink4a/Arf$^{-/-}$ astrocytes). None of the CD31$^+$ cells expressed EGFP, whereas all Nestin$^+$, Tuj1$^+$, or NG2$^+$ tumor cells were EGFP$^+$ (data not shown), indicating that these cells are derived from the injected Id4-transduced Ink4a/Arf$^{-/-}$ astrocytes. The same marker profiles were observed in tumor cells derived from subcutaneous injection of Id4-transduced Ink4a/Arf$^{-/-}$ astrocytes (Cd133$^+$, Nestin$^+$, or Tuj1$^+$ cells) (Supplemental Fig. S5B). Notably, most Tuj1$^+$ cells did not express Cd133 or Nestin, and were closely associated with Cd133$^+$ or Nestin$^+$ cells. In contrast to the Id4-transduced cells, the vector-transduced control cells failed to produce tumors and coimmunofluorescence using Tuj1/EGFP, NG2/EGFP, and GFAP/EGFP antibodies did not show consistent colocalization patterns for the residual EGFP$^+$ cells (data not shown). Thus, tumor cells derived from Id4-transduced Ink4a/Arf$^{-/-}$ astrocytes express an array of lineage markers consistent with astrocyte dedifferentation to an immature NSC/progenitor state with multilineage potential and developmental plasticity.

Cyclin E contributes to elevated growth rate and tumorigenicity of Id4-transduced Ink4a/Arf$^{-/-}$ astrocytes

The exuberant growth rates associated with Id4 transduction prompted analysis of cell cycle-positive and -negative regulatory factors, resulting in documentation of increased nuclear cyclin E and hyperphosphorylated Rb in Id4-transduced Ink4a/Arf$^{-/-}$ astrocytes relative to controls (Fig. 3A–C). Next, gain- and loss-of-function studies revealed that cyclin E transduction increased proliferation in vector-transduced Ink4a/Arf$^{-/-}$ astrocytes (Fig. 3D) to rates comparable with those of Id4-transduced Ink4a/Arf$^{-/-}$ astrocytes (Supplemental Fig. S1D). Reciprocally, shRNA-mediated depletion of cyclin E caused markedly decreased proliferation of Id4-transduced Ink4a/Arf$^{-/-}$ astrocytes (Fig. 3E). These findings are in line with a prolonged G1/S profile in the Id4 deficient embryonic dorsal telencephalon (Yun et al. 2004). In tumor studies, cyclin E overexpression in Ink4a/Arf$^{-/-}$ astrocytes resulted in tumor formation, although these tumors were smaller in size than those generated from Id4-transduced Ink4a/Arf$^{-/-}$ astrocytes (Fig. 3F). Conversely, shRNA-mediated depletion of cyclin E in Id4-transduced Ink4a/Arf$^{-/-}$ astrocytes resulted in signifi-

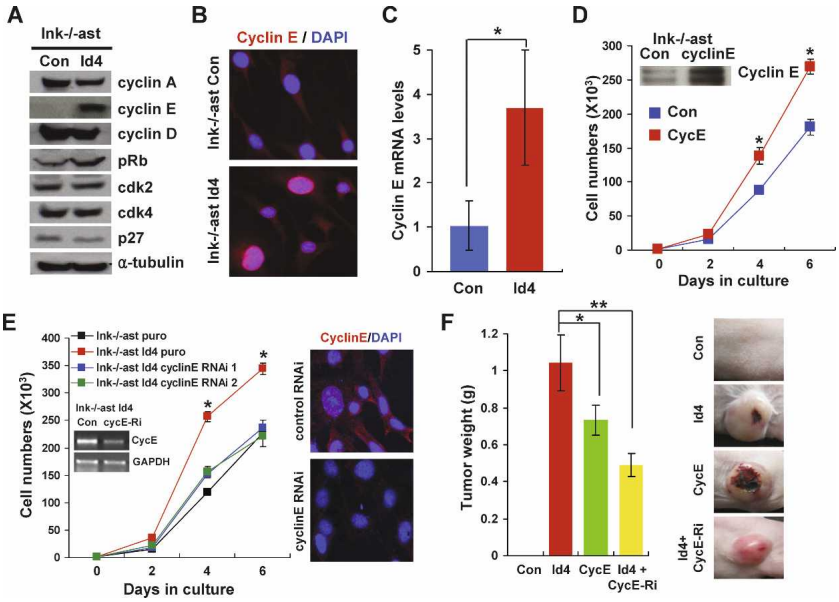

Figure 3. Overexpression of cyclin E in the Id4 overexpressing Ink4a/Arf$^{-/-}$ astrocytes is responsible for elevated growth rate and tumorigenicity. (*A*) Expression of a variety of cell cycle regulators in the vector-transduced Ink4a/Arf$^{-/-}$ astrocytes and Id4-transduced Ink4a/Arf$^{-/-}$ astrocytes was determined by Western blot analysis. (*B*) Expression of cyclin E protein in the vector-transduced Ink4a/Arf$^{-/-}$ astrocytes and Id4-transduced Ink4a/Arf$^{-/-}$ astrocytes was determined by immunofluorescence. (*C*) Cyclin E mRNA levels in the vector-transduced Ink4a/Arf$^{-/-}$ astrocytes and Id4-transduced Ink4a/Arf$^{-/-}$ astrocytes were determined by real-time RT–PCR. (*) $P < 0.05$. (*D*) In vitro growth rate of vector-transduced Ink4a/Arf$^{-/-}$ astrocytes and cyclin E-transduced Ink4a/Arf$^{-/-}$ astrocytes. (*Inset*) Expression levels of cyclin E in these cells were determined by Western blot analysis. (*) $P < 0.01$. (*E*) In vitro growth inhibition of Id4-transduced Ink4a/Arf$^{-/-}$ astrocytes that were subjected to down-regulation of cyclin E through cyclin E-specific shRNA (cyclin E RNAi). Expression levels of cyclin E in these cells were determined by semiquantitative RT–PCR (*inset*) and immunofluorescence (*right* panel). (*) $P < 0.01$. (*F*) Decreased in vivo tumor growth via down-regulation of cyclin E in the Id4-transduced Ink4a/Arf$^{-/-}$ astrocytes. Tumor weight (*left* panel) and representative photos (*right* panel) showing nude mice injected subcutaneously with Ink4a/Arf$^{-/-}$ astrocytes-Con, Ink4a/Arf$^{-/-}$ astrocytes-Id4, Ink4a/Arf$^{-/-}$ astrocytes-cyclin E, and Ink4a/Arf$^{-/-}$ astrocytes-Id4 + cyclin E-shRNA (n = 6). (*) $P < 0.01$; (**) $P < 0.01$.

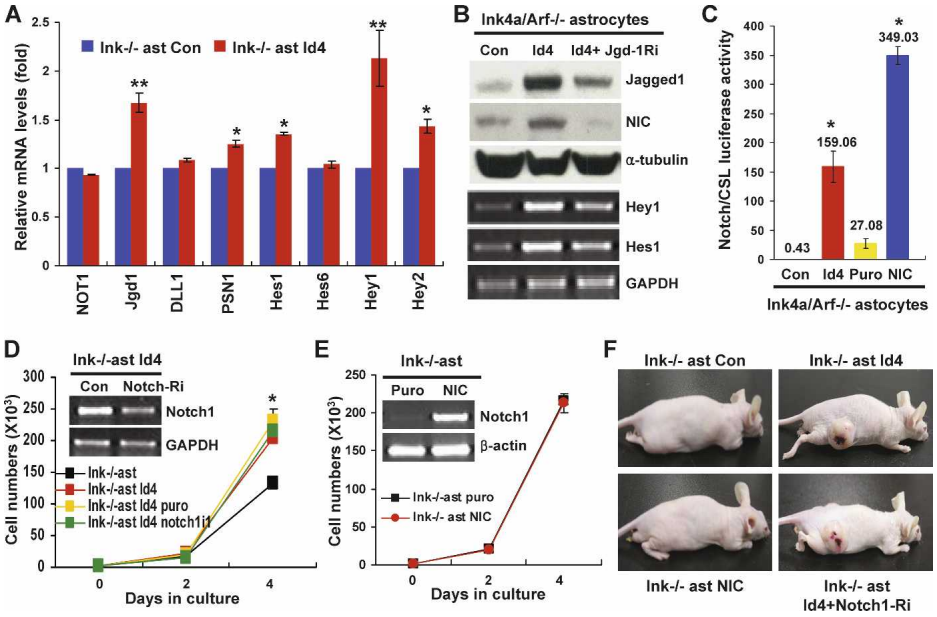

Figure 4. Notch signaling is activated by Id4, but is not associated with tumorigenicity of the Id4-transduced Ink4a/Arf$^{-/-}$ astrocytes. (*A*) Expression levels of genes relative to Notch signaling were determined by semiquantitative RT–PCR. (*) $P < 0.01$; (**) $P < 0.01$. (*B*) Expression levels of Jagged1 and active Notch1 in the Ink4a/Arf$^{-/-}$ astrocytes-Con, Ink4a/Arf$^{-/-}$ astrocytes-Id4, and Ink4a/Arf$^{-/-}$ astrocytes-Id4 + Jagged1-shRNA were determined by Western blot analysis. α-Tubulin was used as a loading control. Expression levels of Hey1 and Hes1 (Notch-downstream genes) in these cells were determined by semiquantitative RT–PCR. GAPDH was used as a loading control. (*C*) Relative Notch transcriptional activity in the Ink4a/Arf$^{-/-}$ astrocytes-Con, Ink4a/Arf$^{-/-}$ astrocytes-Id4, Ink4a/Arf$^{-/-}$ astrocytes-Puro, and Ink4a/Arf$^{-/-}$ astrocytes-NIC was determined by Notch/CSL luciferase-reporter assay. (*) $P < 0.01$. (*D*) Cell proliferation rate of Ink4a/Arf$^{-/-}$ astrocytes-Id4 and Ink4a/Arf$^{-/-}$ astrocytes-Id4 + Notch1-shRNA. (*Inset*) Expression levels of Notch1 in these cells were determined by semiquantitative RT–PCR. (*) $P < 0.01$. (*E*) Cell proliferation rates of Ink4a/Arf$^{-/-}$ astrocytes-Puro, and Ink4a/Arf$^{-/-}$ astrocytes-NIC. (*Inset*) Expression levels of active NIC in these cells were determined by semiquantitative RT–PCR. (*F*) Representative photos showing nude mice ($n = 6$) subcutaneously injected with Ink4a/Arf$^{-/-}$ astrocytes-Con, Ink4a/Arf$^{-/-}$ astrocytes-Id4, Ink4a/Arf$^{-/-}$ astrocytes-NIC, and Ink4a/Arf$^{-/-}$ astrocytes-Id4 + Notch1-shRNA.

cant inhibition of tumor growth with an associated decrease in tumor cell proliferation as judged by PCNA staining (Fig. 3F; Supplemental Fig. S6A). Finally, a link between Id4 and cyclin E was further supported by colocalized expression in human GBM specimens (Supplemental Fig. S6B). Our cyclin E findings gain added significance in light of previous studies establishing a positive correlation between increased cyclin E levels and poor prognosis in brain tumors (Tamiya et al. 2001). Thus, oncogenic activity of Id4 appears to be executed in part through cyclin E-driven cell proliferation.

Id4 overexpression activates Notch signaling

Notch activation has been shown to be integral to stem cell renewal (Chiba 2006), the control of neuronal cell fate (Louvi and Artavanis-Tsakonas 2006), and the malignant transformation of many cancers particularly lymphoid cells (Grabher et al. 2006; Hansson et al. 2004). The dedifferentiation profile and NSC-like phenotype of Id4-transduced cells prompted us to examine components of the Notch signaling pathway (Artavanis-Tsakonas et al. 1999). Relative to vector-transduced controls, Jagged1, Presenilin-1, Hes1, Hey1, and Hey3 levels were significantly increased in Id4-transduced Ink4a/Arf$^{-/-}$ astrocytes, whereas Delta-like 1 and Hes6 expression levels were comparable (Fig. 4A). While Notch1 levels were unchanged, Id4 overexpressing cells showed markedly increased levels of activated Notch1 (NIC; Notch intracellular domain) (Fig. 4B; Supplemental Fig. S7A), as well as increased Notch/CSL luciferase reporter activity (Fig. 4C). The high levels of the Notch1 ligand, Jagged1, prompted analysis of Notch1 downstream signaling following shRNA-mediated depletion of Jagged1 in Id4-transduced Ink4a/Arf$^{-/-}$ astrocytes. Jagged1 knockdown resulted in decreased expression of NIC and its downstream targets, Hey1 and Hes1 (Fig. 4B). The relevance of Jagged1–Notch signaling in GBM pathogenesis is further supported by colocalization of Id4 and Notch1 in human GBM specimens (Supplemental Fig. S7B).

Next, we assessed the pathogenetic contributions of activated Notch1 to Id4-induced gliomagenesis. shRNA-mediated Notch1 depletion in Id4-transduced Ink4a/Arf$^{-/-}$ astrocytes or NIC overexpression in Ink4a/Arf$^{-/-}$ astrocytes had no impact on proliferation rates (Fig. 4D,E; Supplemental Fig. S8). Furthermore, NIC overexpressing Ink4a/Arf$^{-/-}$ astrocytes were nontumorigenic and, reciprocally, Notch1 knockdown (80%) did not inhibit the tumorigenic potential of Id4-transduced Ink4a/Arf$^{-/-}$ astrocytes ($n = 6$ mice) (Fig. 4F), suggesting that Notch1 does not play a direct role in the establishment of tumors from Id4-transduced Ink4a/Arf$^{-/-}$ astrocytes.

Id4-activated Notch signaling, but not cyclin E, is required to maintain the neural stem-like cell properties of the Ink4a/Arf$^{-/-}$ astrocytes

We next examined the impact of activated Notch signaling on the immature differentiation profiles and neurosphere-forming capacity of Id4-transduced Ink4a/Arf$^{-/-}$ astrocytes. Notch1, but not cyclin E, knockdown resulted in a marked decrease in the expression of NSC markers, Nestin, Cd133, and Hes1, and correspondingly,

NIC overexpression in Ink4a/Arf$^{-/-}$ astrocytes induced expression of these immature markers (Fig. 5A). In the neurosphere assay, Notch1 knockdown resulted in a significant decrease in neurosphere number from the Id4-transduced Ink4a/Arf$^{-/-}$ astrocytes compared with a modest decrease in the cyclin E knockdown cultures (Fig. 5B). Furthermore, NIC overexpression, but not cyclin E, was comparable with Id4 in promoting neurosphere formation following their transduction into Ink4a/Arf$^{-/-}$ astrocytes (Fig. 5C). Pharmacological inhibition of Notch signaling (DAPT, a γ-secretase inhibitor) or Jagged1 knockdown in Id4-transduced Ink4a/Arf$^{-/-}$ astrocytes resulted in decreased neurosphere-forming capacity and NSC marker expression (Supplemental Fig. S9A–C). Thus, Id4-induced activation of Jagged–Notch axis in Ink4a/Arf$^{-/-}$ astrocytes plays an essential role in promoting the neural stem cell-like phenotype.

Id4-dependent Notch signaling and cyclin E expression in the human glioma cell lines

Next, we sought to corroborate the murine findings in human glioma cells. shRNA-mediated depletion of Id4 in human LN229 glioma cells (which express the highest levels of Id4) (Supplemental Fig. S1B) resulted in down-regulation of cyclin E, Jagged1, NIC, Notch-downstream target genes (Hes1, Hey1, and Hey2), and Notch transcriptional activity, as well as a marked decrease in cell proliferation (Supplemental Fig. S10A–C). Conversely, Id4 overexpression in human A172 glioma cells (which express low endogenous levels of Id4) induced up-regulation of Jagged1, NIC, and cyclin E; Notch transcriptional activity; cell proliferation; and neurosphere formation (Supplemental Fig. S10D–F). We also found that expression levels of Id4, NIC, Jagged1, and cyclin E were markedly increased in the primary human glioma stem cell line, NCI0822 (Lee et al. 2008), as compared with NHA and HB1.F3 cells (Supplemental Fig. S10G).

Furthermore, we used a Tet-On-inducible gene expression system to assess whether Id4 directly leads to induction of cyclin E and Notch signaling. As shown in Supplemental Fig. S10H, Id4 was markedly increased in the Ink4a/Arf$^{-/-}$ astrocytes transduced with rtTA and Rev-TRE-Id4 grown in the presence of doxycycline (Dox) for 2 d compared with Dox-untreated counterpart cells. We also found that Dox-treated cells showed marked elevations in the levels of cyclin E, Jagged1, and NIC. These results strengthen the link between Id4 and the control of cyclin E and Notch signaling in the astrocytes.

In conclusion, our findings that Id4 can drive the malignant transformation of astrocytes via disregulation of cell cycle and differentiation control, achieved through the up-regulation of cyclin E and activation of Jagged-Notch1 signaling. These findings of Id4-induced developmental plasticity have implications for both the cellular origins of GBM as well as its prominent renewal potential in experimental and clinical trials setting. Thus, these observations may inform the rational development of anti-Id4 agents that may impede the insuperable nature of GBM recurrence.

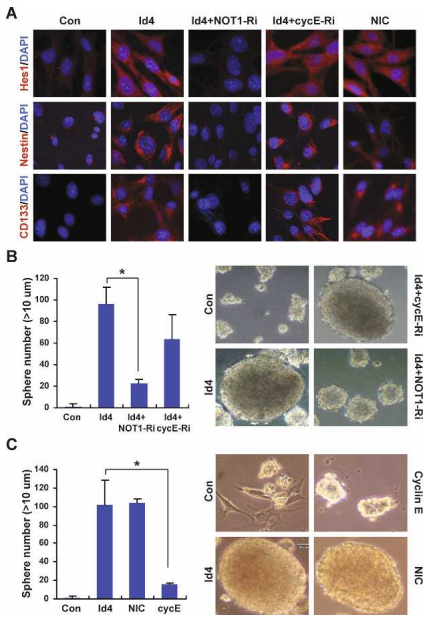

Figure 5. Id4-activated Notch signaling, but not cyclin E expression, is required to maintain the neural stem-like cell properties of the Ink4a/Arf$^{-/-}$ astrocytes. (*A*) Immunofluorescence images (400× magnification) of Hes1 (Notch signaling marker), Nestin, and CD133 (neural stem and progenitor cell markers) in the Ink4a/Arf$^{-/-}$ astrocytes-Con, Ink4a/Arf$^{-/-}$ astrocytes-Id4, Ink4a/Arf$^{-/-}$ astrocytes--Id4 + Notch1-shRNA, Ink4a/Arf$^{-/-}$ astrocytes-Id4 + cyclin E-shRNA, and Ink4a/Arf$^{-/-}$ astrocytes-NIC grown in DMEM + 10% FBS culture conditions. (*B*, *left* panel) Number of neurospheres (>10 µm) generated from Ink4a/Arf$^{-/-}$ astrocytes-Con, Ink4a/Arf$^{-/-}$ astrocytes-Id4, Ink4a/Arf$^{-/-}$ astrocytes-Id4 + cyclin E-shRNA, and Ink4a/Arf$^{-/-}$ astrocytes-Id4 + Notch1-shRNA (4000 cells per 24-well plate) grown in neural stem cell cultures for 10 d. (*Right* panel) Representative photos (40×) showing the morphologies of cells grown in neural stem cell cultures. (*) $P < 0.01$. (*C*, *left* panel) Number of neurospheres (>10 µm) generated from Ink4a/Arf$^{-/-}$ astrocytes-Con, Ink4a/Arf$^{-/-}$ astrocytes-Id4, Ink4a/Arf$^{-/-}$ astrocytes-cyclin E, and Ink4a/Arf$^{-/-}$ astrocytes-NIC (4000 cells per 24-well plate) grown in neural stem cell cultures for 10 d. (*Right* panel) Representative photos (40×) showing the morphologies of cells grown in neural stem cell cultures. (*) $P < 0.01$.

Materials and methods

Cell culture and conditions

Mouse astrocytes were isolated from the cerebral cortices of 5-d-old Ink4a/Arf$^{-/-}$ knockout mice as described previously (Bachoo et al. 2002). Ink4a/Arf$^{-/-}$ astrocytes and human GBM cell lines were maintained in Dulbecco's modified Eagle's medium (DMEM) enriched with 10% fetal bovine serum (Hyclone), 1% penicillin, and streptomycin (GIBCO-BRL), and 2 mM L-glutamine (GIBCO-BRL). For neural sphere formation, cells (a single cell in each well of a 96-well plate or 200 cells in a 24-well plate, which corresponds to one cell per square millimeter) were maintained in neural stem cell (NSC) culture conditions (DMEM/F12 medium enriched with 20 ng/mL EGF, 20 ng/mL bFGF, 1× B27) and 1% penicillin and streptomycin for 7–10 d as described previously, with minor modification (Lee et al. 2006).

Full materials and methods are available in the Supplemental Material.

Acknowledgments

We thank Seung U. Kim for human neural stem cell (HB1.F3), Howard A. Fine for human glioma stem cell (NCI0822), and Eui-Ju Choi for the Notch/CSL luciferase–reporter construct. This work was supported by a grant from the National R&D Program for Cancer Control, Ministry of Health and Welfare, Republic of Korea (0720030 to H.K.), and NIH grants (RO1CA99041 to L.C. and PO1CA95616 to R.A.D. and L.C.). R.A.D. is an American Cancer Society Research Professor and an Ellison Medical Foundation Scholar and is supported by the Robert A. and Renee E. Belfer Foundation Institute for Innovative Cancer Science.

References

Artavanis-Tsakonas, S., Rand, M.D., and Lake, R.J. 1999. Notch signaling: Cell fate control and signal integration in development. *Science* **284:** 770–776.

Bachoo, R.M., Maher, E.A., Ligon, K.L., Sharpless, N.E., Chan, S.S., You, M.J., Tang, Y., DeFrances, J., Stover, E., Weissleder, R., et al. 2002. Epidermal growth factor receptor and Ink4a/Arf: Convergent mechanisms governing terminal differentiation and transformation along the neural stem cell to astrocyte axis. *Cancer Cell* **1:** 269–277.

Beachy, P.A., Karhadkar, S.S., and Berman, D.M. 2004. Tissue repair and stem cell renewal in carcinogenesis. *Nature* **432:** 324–331.

Bedford, L., Walker, R., Kondo, T., van Crüchten, I., King, E.R., and Sablitzky, F. 2005. Id4 is required for the correct timing of neural differentiation. *Dev. Biol.* **280:** 386–395.

Calabrese, C., Poppleton, H., Kocak, M., Hogg, T.L., Fuller, C., Hamner, B., Oh, E.Y., Gaber, M.W., Finklestein, D., Allen, M., et al. 2007. A perivascular niche for brain tumor stem cells. *Cancer Cell* **11:** 69–82.

Chiba, S. 2006. Notch signaling in stem cell systems. *Stem Cells* **24:** 2437–2447.

Cho, T., Bae, J.H., Choi, H.B., Kim, S.S., McLarnon, J.G., Suh-Kim, H., Kim, S.U., and Min, C.K. 2002. Human neural stem cells: Electrophysiological properties of valtage-gated ion channels. *Neuroreport* **13:** 1447–1452.

Galli, R., Binda, E., Orfanelli, U., Cipelletti, B., Gritti, A., De Vitis, S., Fiocco, R., Foroni, C., Dimeco, F., and Vescovi, A. 2004. Isolation and characterization of tumorigenic, stem-like neural precursors from human glioblastoma. *Cancer Res.* **64:** 7011–7021.

Garraway, L.A. and Sellers, W.R. 2006. Lineage dependency and lineage-survival oncogenes in human cancer. *Nat. Rev. Cancer* **6:** 593–602.

Grabher, C., von Boehmer, H., and Look, A.T. 2006. Notch 1 activation in the molecular pathogenesis of T-cell acute lymphoblastic leukaemia. *Nat. Rev. Cancer* **6:** 347–359.

Hansson, E.M., Lendahl, U., and Chapman, G. 2004. Notch signaling in development and disease. *Semin. Cancer Biol.* **14:** 320–328.

Jen, Y., Manova, K., and Benezra, R. 1996. Expression patterns of Id1, Id2, and Id3 are highly related but distinct from that of Id4 during mouse embryogenesis. *Dev. Dyn.* **207:** 235–252.

Keller, G. 2005. Embryonic stem cell differentiation: Emergence of a new era in biology and medicine. *Genes & Dev.* **19:** 1129–1155.

Lee, J., Kotliarova, S., Kotliarov, Y., Li, A., Su, Q., Donin, N.M., Pastorino, S., Purow, B.W., Christopher, N., Zhang, W., et al. 2006. Tumor stem cells derived from glioblastomas cultured in bFGF and EGF more closely mirror the phenotype and genotype of primary tumors than do serum-cultured cell lines. *Cancer Cell* **9:** 391–403.

Lee, J., Son, M.J., Woolard, K., Donin, N.M., Li, A., Cheng, C.H., Kotliarova, S., Kotliarov, Y., Walling, J., Ahn, S., et al. 2008. Epigenetic-mediated dysfunction of the bone morphogenetic protein pathway inhibits differentiation of glioblastoma-initiating cells. *Cancer Cell* **13:** 69–80.

Leung, C., Lingbeek, M., Shakhova, O., Liu, J., Tanger, E., Saremaslani, P., Van Lohuizen, M., and Marino, S. 2004. Bmi1 is essential for cerebellar development and is overexpressed in human medulloblastomas. *Nature* **428:** 337–341.

Ligon, K.L., Huillard, E., Mehta, S., Kesari, S., Liu, H., Alberta, J.A., Bachoo, R.M., Kane, M., Louis, D.N., Depinho, R.A., et al. 2007. Olig2-regulated lineage-restricted pathway controls replication competence in neural stem cells and malignant glioma. *Neuron* **53:** 503–517.

Louvi, A. and Artavanis-Tsakonas, S. 2006. Notch signaling in vertebrate neural development. *Nat. Rev. Neurosci.* **7:** 93–102.

Lyden, D., Young, A.Z., Zagzag, D., Yan, W., Gerald, W., O'Reilly, R., Bader, B.L., Hynes, R.O., Zhuang, Y., Manova, K., et al. 1999. Id1 and Id3 are required for neurogenesis, angiogenesis and vascularization of tumour xenografts. *Nature* **401:** 670–677.

Pardal, R., Clarke, M.F., and Morrison, S.J. 2003. Applying the principles of stem-cell biology to cancer. *Nat. Rev. Cancer* **3:** 895–902.

Singh, S.K., Hawkins, C., Clarke, I.D., Squire, J.A., Bayani, J., Hide, T., Henkelman, R.M., Cusimano, M.D., and Dirks, P.B. 2004. Identification of human brain tumour initiating cells. *Nature* **432:** 396–401.

Tamiya, T., Mizumatsu, S., Ono, Y., Abe, T., Matsumoto, K., Furuta, T., and Ohmoto, T. 2001. High cyclinE/low p27Kip1 expression is associated with poor prognosis in astrocytomas. *Acta Neuropathol. (Berl.)* **101:** 334–340.

Vescovi, A.L., Galli, R., and Reynolds, B.A. 2006. Brain tumour stem cells. *Nat. Rev. Cancer* **6:** 425–436.

Yun, K., Mantani, A., Garel, S., Rubenstein, J., and Israel, M.A. 2004. Id4 regulates neural progenitor proliferation and differentiation *in vivo*. *Development* **131:** 5441–5448.

Inhibitor of differentiation 4 drives brain tumor-initiating cell genesis through cyclin E and notch signaling

Hye-Min Jeon, Xun Jin, Joong-Seob Lee, et al.

Genes Dev. 2008, **22:**
Access the most recent version at doi:10.1101/gad.1668708